

Towards High Precision: An Adaptive Self-Supervised Learning Framework for Force-Based Verification

Zebin Duan¹, Frederik Hagelskjær¹, Aljaz Kramberger¹, Juan Heredia¹, Norbert Krüger^{1,2}

Abstract—The automation of robotic tasks requires high precision and adaptability, particularly in force-based operations such as insertions. Traditional learning-based approaches either rely on static datasets, which limit their ability to generalize, or require frequent manual intervention to maintain good performances. As a result, ensuring long-term reliability without human supervision remains a significant challenge. To address this, we propose an adaptive self-supervised learning framework for insertion classification that continuously improves its precision over time. The framework operates in real-time, incrementally refining its classification decisions by integrating newly acquired force data. Unlike conventional methods, it does not rely on pre-collected datasets but instead evolves dynamically with each task execution. Through real-world experiments, we demonstrate how the system progressively reduces execution time while maintaining near-perfect precision as more samples are processed. This adaptability ensures long-term reliability in force-based robotic tasks while minimizing the need for manual intervention.

I. INTRODUCTION

Achieving high precision in force classification of robotic tasks presents a significant challenge. Traditional machine learning approaches require large-scale labeled datasets for supervised training, but manual labeling is often impractical for industrial applications. It is time-consuming, prone to inconsistencies when performed by non-experts, and unsuitable for high-mix low-volume production environments where rapid deployment is essential [1] [2]. To overcome these limitations, self-supervised learning techniques have emerged [3], enabling systems to autonomously generate labels without human intervention.

Force sensing is fundamental for robotic assembly [4], insertion [5], and other contact-based interactions, as it allows robots to adapt to environment variations, detect anomalies [6] and improve task success rates. However, force measurements are highly sensitive to external factors such as temperature, friction and surface variations, making it challenging to develop accurate force-based classification models without real-world data. While simulations are widely used in robotics [7], accurately modeling force interactions introduces significant complexity, reinforcing the necessity of real-world data for robust learning.

To achieve high precision in classification tasks without relying on tedious manual labeling and simulations, we introduce an adaptive self-supervised learning framework that

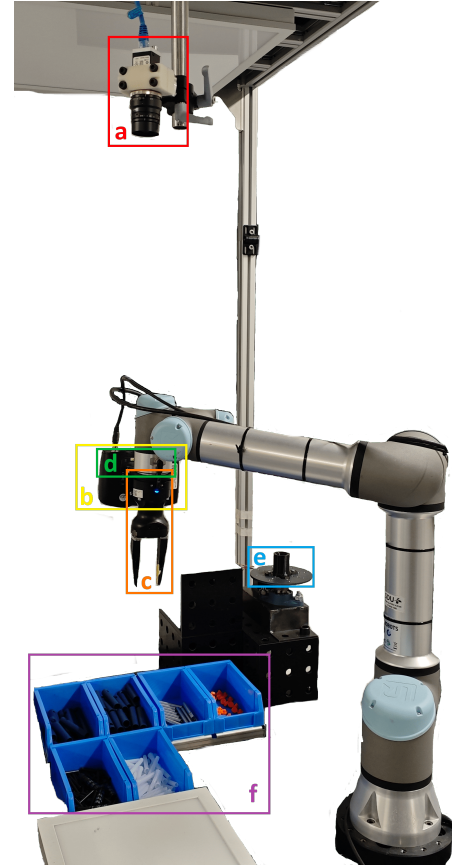


Fig. 1: Work cell setup consisting of the following components: (a) 2D camera positioned above the work cell for auxiliary top-down view, (b) 3D camera mounted on the gripper for vision-based tasks, (c) Gripper with two fingers for object manipulation (d) Force-Torque sensor built in the robot end-effector (e) Fixture on top of a rotating table where the object will be inserted (f) Bins containing the test objects.

leverages force data. The framework incrementally improves insertion classification performances by continuously updating its model during execution. This approach eliminates the need for offline retraining, pre-collected datasets or manual annotations. The system is tested using a bin picking work cell described in Fig. 1 and the workflow pipeline of Fig. 2. Unlike static models, our approach starts with minimal prior knowledge and refines its decision-making as new force data become available, progressively reducing misclassifications.

Our work demonstrates how force-torque sensors can be utilized to develop self-improving robotic workflows without

¹All authors are with the Mærsk Mc-Kinney Møller Institute, University of Southern Denmark, 5230 Odense M, Denmark. {zeb, frhag, alk, jehm, norbert}@mmmi.sdu.dk

²The author is affiliated with the Danish Institute for Advanced Study (DIAS), University of Southern Denmark, 5230 Odense M, Denmark. norbert@mmmi.sdu.dk

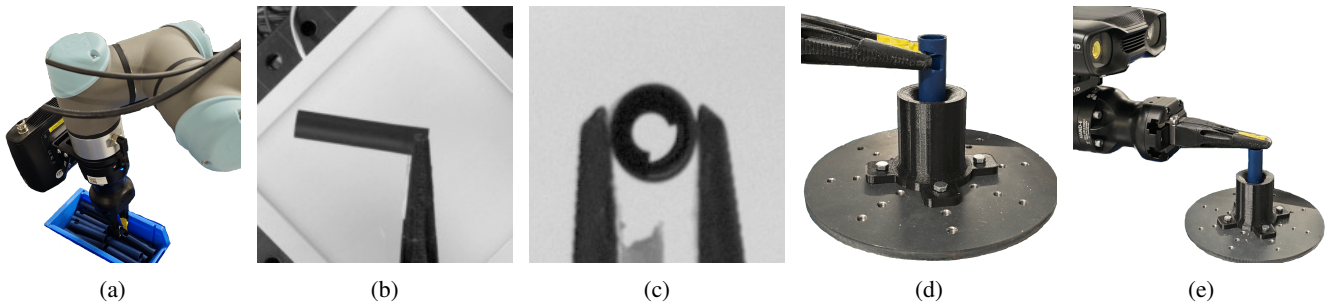


Fig. 2: The pipeline of our system: (a) Object pose estimation and bin picking of the object. (b) In-hand pose estimation (c) Revolution estimation from top-down view (d) Insertion of the object into the fixture. (e) Height verification.

additional infrastructure or costly validation steps. By applying an adaptive classification rule (Sec. III-C), the proposed framework allows robots to autonomously perform insertion tasks while enhancing performance over time.

Specifically, our contributions include:

- A method for dynamically improving insertion classification by continuously refining force-based decision-making.
- A self-supervised learning approach that enables long-term precision improvement in force classification tasks.
- Real-world experiments validating the system’s ability to progressively enhance precision with each execution.

The remainder of this paper details related works Sec. II, the methodology Sec. III, the experimental evaluation Sec. IV, and conclusions Sec. V.

II. RELATED WORK

Robotic insertion and assembly tasks pose persistent challenges due to the challenges of achieving both high precision and robust performance in uncertain environments. While progress in grasping has improved object acquisition, precise insertion remains significantly more sensitive to small errors, requiring robust feedback mechanisms and adaptive learning strategies.

Force based monitoring and verification have been widely explored for insertion tasks. In industrial contexts, force-torque sensing is commonly used to detect deviations or insertion failures, as shown by Lee et al. [4], who monitor characteristic force profiles during component alignment. In surgical robotics, similar principles apply; for example, Pile et al. [8] use force feedback to detect critical failure points during cochlear electrode insertion. Pitchandi et al. [9] focus specifically on peg-in-hole tasks with compliant fixtures, identifying force signatures that differentiate successful from failed insertions. These works emphasize the importance of multimodal feedback, integrating force and tactile sensing, to enhance fault prediction in robotic solutions.

Learning-based approaches have sought to generalize such force-torque driven verification. Zhou et al. [10] train supervised models on force-torque data to classify stacking outcomes, while Papavasileiou et al. [11] apply decision trees for contact-based quality control. However, such approaches

often require extensive labeled datasets and may not adapt well to unseen configurations.

To mitigate these limitations, *Self-supervised learning* has gained significant attention in robotic automation due to its ability to reduce reliance on manual labeling, allowing systems to continuously improve by learning directly from their own experiences. Berscheid et al. [12] emphasize how this approach minimizes human supervision, particularly in robotic grasping tasks, where it enhances pose estimation and improves success rates over time. In robotic perception, self-supervised learning has been applied to visual modalities [13], but only limited attention has been paid to self-supervised learning on force data. Moreover, [14] proposed an online learning framework for robotic grasp adaptation, though it lacked real-time force-based verification.

Although previous work has explored *force sensing* and *self-supervised learning* independently, few studies have combined these approaches for real-time robotic verification. Our work builds upon these studies by applying self-supervised learning to force data in insertion tasks, enabling the system to refine its predictions autonomously and continuously enhance its performance dynamically to new instances.

III. METHODOLOGY

A. System overview

The workflow pipeline is shown in Fig. 2. The system is based on the improved bin-picking work cell of [15] introduced in [16]. In the first stage, the system captures a 3D point cloud of the scene, estimates the poses of objects inside the bin, and computes grasp poses as seen in Fig. 2(a). A grasp attempt is then performed, placing the object in the robot’s fingers. This is followed by in-hand pose estimation as shown in Fig. 2(b), which corrects any misalignment that may have occurred during grasping. Finally, the object is placed into a fixture based on the found pose estimate.

For the object addressed in this paper, the in-hand pose estimation is inadequate. To insert the object correctly into the fixture, the full 6 Degrees of Freedom pose estimate should be known. However, the correct orientation of the object is uncertain given the view of the in-hand pose estimation, see 2(b). To determine the revolution of the object, a second in-hand pose estimation is performed, where

the object is rotated to present a view of the internal structure, see Fig. 2(c). This rotation is based on the initial in-hand pose estimate. The second in-hand pose estimate is performed using the same template matching as the initial in-hand pose estimate [17]. The object is then placed into the fixture, where the fixture has been placed on a rotating table allowing the object to be placed in the correct orientation as seen in Fig. 2(d). Lastly, the system performs a height verification to classify the insertion as successful or unsuccessful Fig. 2(e).

Unlike [16], during the insertion step in Fig. 2(d), we continuously record force data from the force-torque sensor, enabling immediate classification of the insertion upon completion using the classification algorithm based on k -NN and l -Value voting rule described in Sec. III-C. The time-cost height verification method in Fig. 2(e) is only triggered when the model’s prediction is uncertain, reducing the need for this additional verification step and optimizing overall processing time.

The test object used in our experiments is illustrated in Fig. 3. It has a single lateral hole, and the insertion success is determined based on the object’s post-insertion height. Specifically, when the lateral hole is positioned on the top side after insertion, the object’s height is lower compared to when the hole is on the bottom side. In this case, the insertion is classified as positive; otherwise, it is considered negative. The hole’s position can also be inferred from a top-down view as we can see from Fig. 2(c). However, this approach only determines the lateral hole’s correct position without indicating whether it is on the top or bottom of the cylindrical object. In our experiments, we will only consider the forces in the z-axis as the main movement is along the z direction.

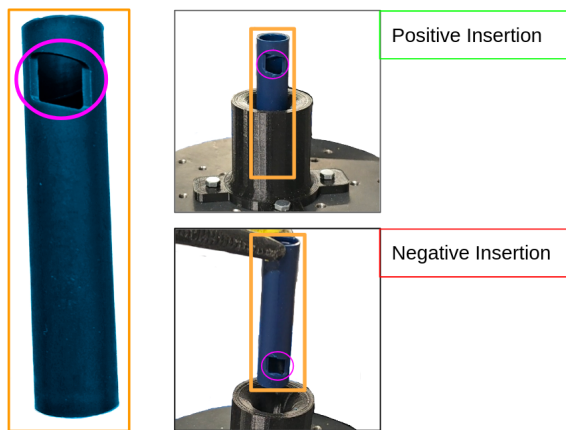


Fig. 3: Test object overview, part of an injection device

B. Data Collection Characteristics

Force data was recorded at 500 Hz over a 2-second interval, resulting in 1000-dimensional feature vectors. To mitigate sensor noise, we applied a Savitzky-Golay filter [18] with $window_size = 15$ and $polynomial_order = 2$, which effectively preserves force peaks while attenuating high-frequency noise as we can see from Fig. 4. Finally, to reduce

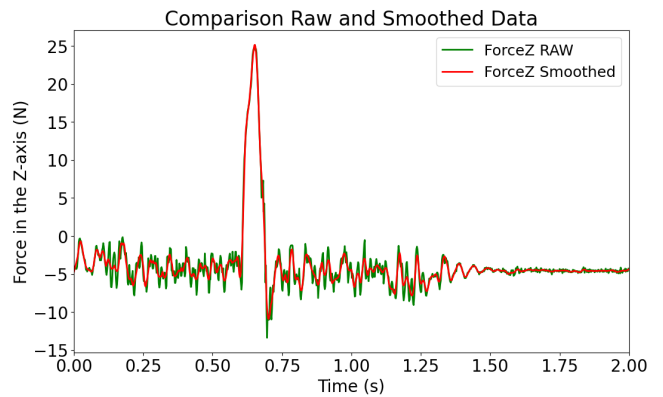


Fig. 4: Denoising effect of the Savitzky-Golay filter on a negative insertion force profile.

the dimensionality of the feature vectors, we employed a sliding window mean down-sampling approach.

C. k -NN and l -Value voting rule

With the collected time-series force data we implement the k -Nearest Neighbors (k -NN) algorithm from Scikit-Learn [19] for this task. Upon receiving a new data point, the k -NN algorithm computes its distance to all points in the training dataset using a distance metric, typically the euclidean distance. The algorithm then identifies the k nearest points in the feature space, where k is a user-defined parameter. The class label most frequent among these k neighbors is assigned to the new data point. The selection of k and the distance metric plays a critical role in the performance of the algorithm. A smaller k value may make the model more sensitive to noise, while a larger k value can lead to a smoother decision boundary.

While k -NN classification traditionally relies on a majority voting mechanism, we propose a modified decision rule that incorporates a minimum agreement threshold, denoted as the l -Value. Specifically, the l -Value requires a predefined percentage of the k neighbors to agree on the same class label for a prediction to be accepted. For example, a l -Value of 90% requires that at least 90% of the nearest neighbors must agree on the classification outcome. If this consensus threshold is not met, the system abstains from making a definitive prediction and instead defaults to the verification process outlined in Fig. 2(e) for final validation.

Mathematically, the modified decision rule can be expressed as:

$$\frac{N_c}{k} * 100 \geq l\% \quad (1)$$

where N_c is the number of neighbors that agree on the class label, k is the total number of nearest neighbors, and l is the l -Value (expressed as a percentage).

For instance, with $k = 11$, at least 10 neighbors must agree on the classification outcome for l -Value of 90%, that is $N_c \geq 9.9$.

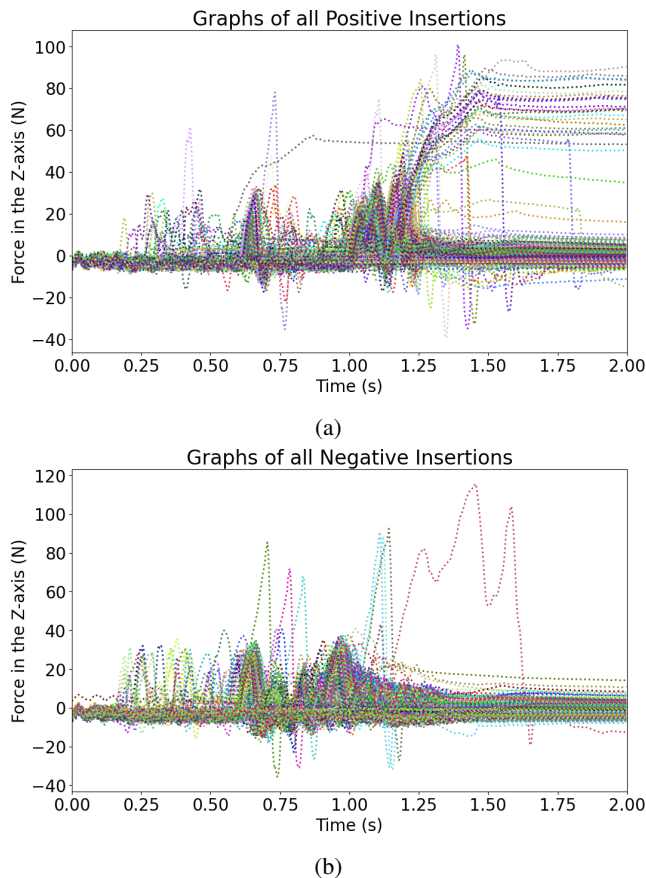


Fig. 5: All force data profiles along the z-axis over time, divided by their class: (a) Positive insertions and (b) Negative insertions.

In this study, we set a fixed $k = 11$ to maintain consistency and simplicity in the classification process, avoiding the added complexity of optimizing k . Additionally, given the high-dimensional nature of our feature vector, we opted for cosine distance instead of the euclidean distance. Cosine distance is well-suited for high-dimensional data and performs effectively with sparse data, as observed in Fig. 5 and from the results in Tab. III.

IV. EXPERIMENTAL EVALUATION

A. Datasets

We collected a total of 704 insertion trials shown in Fig. 5, comprising 297 positive insertions and 407 negative insertions. Of these, 604 trials were used for training and validation, while the remaining 100 were set aside for testing.

B. Evaluation metrics

We evaluated our model using precision and recall Eq. 2, which are defined in terms of True Positives (TP), True Negatives (TN), False Positives (FP) and False Negatives (FN), and described in Tab. I:

$$Precision = \frac{TP}{TP + FP} \quad (2)$$

$$Recall = \frac{TP}{TP + FN}$$

TABLE I: Confusion Matrix for Insertion Classification

	Actual Positive	Actual Negative
Predicted Positive	TP: Correctly classified positive insertion	FP: Incorrectly classified positive insertion, actual insertion is negative
Predicted Negative	FN: Incorrectly classified negative insertion, actual insertion is positive	TN: Correctly classified negative insertion

Our primary objective is to maximize precision, as this reduces the occurrence of false positives, which could result in assembly defects or safety hazards, potentially affecting subsequent stages of the insertion process. In our specific real case, false positives can lead to malfunctioning injection devices. In contrast, false negatives pose minimal risk, as they only incur a slight time cost for removing the object from the fixture after the insertion. By prioritizing precision, only high-confidence insertions are classified as successful, effectively minimizing the propagation of errors in downstream operations.

C. Performance Evaluation Metrics

We performed experiments by varying the training set size, random seed values, and classification l -Value while preserving the training, validation, and test ratio outlined in Sec. IV-A. The results were then aggregated using the mean function and are presented in Fig. 6.

The increase of training size leads to an improvement in model performance. However, the most notable finding is the significant performance gain achieved by modifying the voting rule, as described in Sec. III-C. This improvement is evident when comparing the first and last rows of the heatmaps in Fig. 6(a)(b)(d)(e). As expected, this enhancement comes at the cost of a higher number of unclassified instances, as illustrated in Fig. 6(c)(f). Specifically, according to the standard voting rule ($l - Value \geq 50\%$), every instance is assigned a label, and so the model is never uncertain about the classification. In contrast ($l - Value \geq 100\%$), when the training size is only 15% of its original size, the model struggles to classify most instances, that is around 73% of either the validation or test set. However, as the training set increases, the number of uncertain classifications decreases, thereby reducing the reliance on the time-cost height verification method as it is shown in Fig. 2(e).

D. Online self-supervised performance

We evaluated our framework in a prototype online environment. The framework was executed 30 times, with the

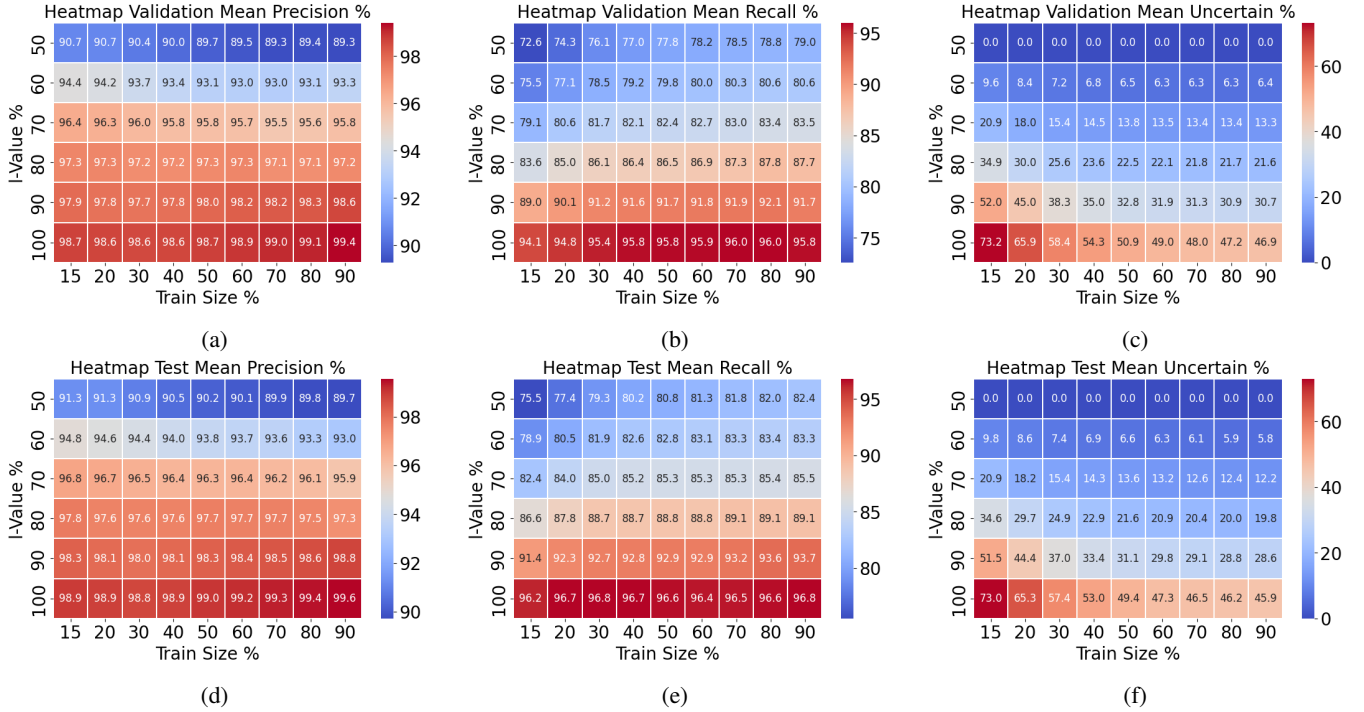


Fig. 6: Heatmap results of evaluation metrics and uncertain percentages for Validation and Test dataset with respect to different training size and l -Value. In order: Validation Set (a) Precision, (b) Recall and (c) Uncertain; Test Set (d) Precision, (e) Recall and (f) Uncertain.

dataset shuffled in each run to ensure variation in the initial base-growing dataset and as if encountering it for the first time from each run. To enhance reliability, final results were averaged across all runs. Each force signal was classified according to the method outlined in Sec. III-C.

Since the k -NN model initially lacks ground truth data, the system employs the height verification method Fig. 2(e) for the first instances. To maintain balance, at least half of this initial dataset consists of positive insertions. These verified samples are then incorporated into the base-growing dataset, enabling subsequent classifications to rely on an expanding reference set.

When the model encounters uncertainty in classification, the height verification method is triggered, and the newly labeled data is added to the base dataset. The model undergoes periodic retraining after a predefined number of classified instances (every 20 in our case), with fixed $k = 11$. After processing all instances, predicted labels were compared against ground truth for evaluation.

Fig. 7(a) illustrates model performance over a sliding window of 100 samples. At each iteration, precision and uncertainty percentages were computed based on the preceding 100 samples. These results indicate that, given the same base training dataset, precision is higher when l -Value = 100% compared to when predicting with l -Value = 50%, although at the cost of increasing reliance on the height verification method. However, as the base-growing dataset expands, the number of uncertain classifications progressively decreases.

Compared to previous work [16], which required the time-

TABLE II: Mean Results of the simulated Online Self-Supervised Learning framework.

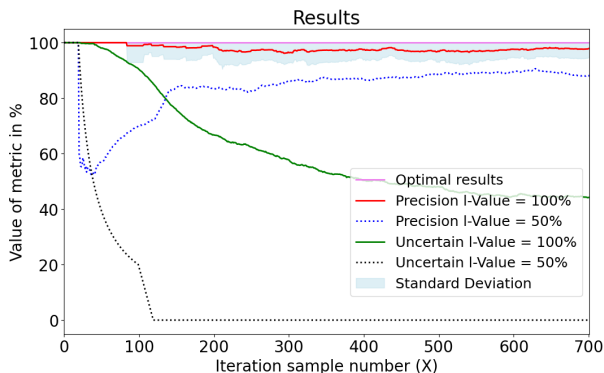
	l -Value = 100%	l -Value = 50%
Samples	704	
Growing Base Dataset size	401.7	
Count Height Verification	401.7	704
Precision	97.72%	83.60%
Recall	94.50%	83.24%
Count of TP	110.2	237.4
Count of FP	2.6	46.8
Count of TN	182.8	351.8
Count of FN	6.4	47.8

intensive height verification step for every instance, our approach significantly reduces its usage.

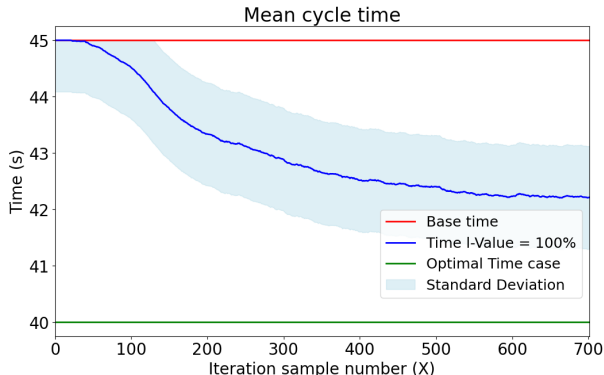
Assuming that the entire pipeline in Fig. 2 takes approximately 45 seconds per iteration, with the height verification step contributing 5 seconds, we obtain the results shown in Fig. 7(b), computed over a sliding window of 100 samples.

The overall classification results across all samples are summarized in Tab. II. On average, our framework eliminates 302.3 out of 704 verification steps, reducing verification by approximately 42.94% and saving a total of 1511 seconds. As such, of the 8 hours 48 minutes needed to record all this data, we could have actually saved around 25 minutes.

Despite this reduction, classification precision remains high. In particular, with l -Value = 100%, false positives instances decrease by 94.44% compared to l -Value = 50%, demonstrating a substantial improvement in classification



(a)



(b)

Fig. 7: Mean results of Online self-supervised framework performances over a sliding windows of 100 samples: (a) Results of Precision and Uncertain samples with different l -Value and (b) Mean cycle time execution.

precision while minimizing unnecessary verification steps.

E. Post-hoc analysis

We performed a small grid search for different parameters in the k -NN context with l -Value = 100% and we obtained the mean results of 30 runs in the prototype online environment in Tab. III. We notice that the best distance metric is the cosine with respect to both precision and the low number of false positives. By using $k = 11$, we can balance between the number of false positives and the number of uncertain instances. This small grid search confirms our parameters choices in Sec. III-C.

V. CONCLUSION

This study serves as an initial investigation into the feasibility of using simple machine learning models to improve classification precision in industrial applications. As demonstrated in Fig. 7, our framework reduces overall cycle time and simultaneously has high precision. These findings highlight the potential of our approach for industrial applications without compromising performance.

Our experimental results demonstrate that integrating force sensing with self-supervised learning significantly reduces

TABLE III: Results of Precision, True Positive, False Positive, True Negative, False Negative and Uncertain samples of the simulated online self-supervised learning framework with different number of k nearest neighbors and metric distance.

K	Metric	Prec.%	TP	FP	TN	FN	Unc.
11	Cosine	97.72%	110.2	2.6	182.8	6.4	401.7
11	Euclidean	91.57%	57.9	5.2	144.6	4.1	491.9
11	Manhattan	83.78%	51.6	11.0	60.2	2.9	578.1
11	Minkowski	92.14%	54.1	4.5	152.0	4.5	488.8
5	Cosine	95.77%	155.4	6.9	257.5	18.6	265.5
11	Cosine	97.72%	110.2	2.6	182.8	6.4	401.7
15	Cosine	97.26%	86.6	2.5	146.3	3.3	465.1
21	Cosine	98.23%	60.2	1.1	106.7	2.4	533.5
25	Cosine	97.48%	59.0	1.56	113.8	2.3	527.2

the usage of costly verification methods in the pipeline workflow as seen in Fig. 2(e).

This approach offers several advantages, including fully automated labeling without human intervention and minimal setup requirements, enabling rapid implementation and deployment, and the system continuously improves its performance as it encounters new instances.

Tab. II shows that, while false positive instances are not entirely eliminated, it is considerably low. Out of a total of 704 samples, only 2.6 were classified as false positives, representing just 0.36% of the full dataset. This outcome is notable, especially considering that several optimization challenges remain unaddressed.

For its simplicity and easy understanding, we opted to use k -NN instead of more complex models. The k -NN algorithm provides greater control over the l -value, making it a practical choice for our framework. However, it would be valuable to compare its performance against deep learning models, particularly in relation to dataset size and generalization capabilities.

Several challenges remain open for future research. First, the selection of the k parameter in k -NN was not rigorously optimized as we used a fixed range of values for the optimal configuration. Second, ensuring the quality of the data added to the growing dataset remains an issue. Although the height verification process provides additional labeled data, not all instances should be incorporated, but only those that enhance classification precision should be retained.

The dataset presented in Fig. 5 reveals significant variations and the presence of outliers in both positive and negative samples. Collecting more data, particularly for rare or outlier cases, could improve model generalization and overall classification performance. Additionally, our pre-processing pipeline (Sec. III-B) may have inadvertently removed important features during the sliding window down-sampling process, or the feature vector may still be too large, impacting efficiency.

To further improve the framework, we plan to:

- Gather more force data of the insertion task.
- Investigate alternative deep learning models to identify the most effective architecture for our case of force-based classification.

- Refine data selection strategies to construct a more efficient and compact dataset, reducing computational overhead while maintaining classification precision.
- Extend the framework to different test objects to evaluate its generalizability.

ACKNOWLEDGMENT

This project was funded in part by Innovation Fund Denmark through the project FERA (3149-00014A), and in part by the SDU I4.0-Lab.

REFERENCES

- [1] O. Russakovsky, J. Deng, H. Su, J. Krause, S. Satheesh, S. Ma, Z. Huang, A. Karpathy, A. Khosla, M. Bernstein, A. C. Berg, and L. Fei-Fei, "ImageNet Large Scale Visual Recognition Challenge," *International Journal of Computer Vision*, vol. 115, no. 3, pp. 211–252, Dec. 2015.
- [2] D. De Gregorio, A. Tonioni, G. Palli, and L. Di Stefano, "Semiautomatic Labeling for Deep Learning in Robotics," *IEEE Transactions on Automation Science and Engineering*, vol. 17, no. 2, pp. 611–620, Apr. 2020, conference Name: IEEE Transactions on Automation Science and Engineering.
- [3] L. Jing and Y. Tian, "Self-Supervised Visual Feature Learning With Deep Neural Networks: A Survey," *IEEE Transactions on Pattern Analysis and Machine Intelligence*, vol. 43, no. 11, pp. 4037–4058, Nov. 2021, conference Name: IEEE Transactions on Pattern Analysis and Machine Intelligence.
- [4] D.-H. Lee, M.-W. Na, J.-B. Song, C.-H. Park, and D.-I. Park, "Assembly process monitoring algorithm using force data and deformation data," *Robotics and Computer-Integrated Manufacturing*, vol. 56, pp. 149–156, Apr. 2019.
- [5] Z. Shen, Z. Jiang, J. Zhang, J. Wu, and Q. Zhu, "Learning-based robot assembly method for peg insertion tasks on inclined hole using time-series force information," *Biomimetic Intelligence and Robotics*, vol. 5, no. 1, p. 100209, 2025.
- [6] S. G. Graabæk, E. V. Ancker, A. R. Fugl, and A. L. Christensen, "An experimental comparison of anomaly detection methods for collaborative robot manipulators," *IEEE Access*, vol. 11, pp. 65 834–65 848, 2023.
- [7] X. Zhang, M. Tomizuka, and H. Li, "Bridging the Sim-to-Real Gap with Dynamic Compliance Tuning for Industrial Insertion," in *2024 IEEE International Conference on Robotics and Automation (ICRA)*, May 2024, pp. 4356–4363.
- [8] J. Pile, G. B. Wanna, and N. Simaan, "Robot-assisted perception augmentation for online detection of insertion failure during cochlear implant surgery," *Robotica*, vol. 35, no. 7, pp. 1598–1615, Jul. 2017.
- [9] N. Pitchandi, S. P. Subramanian, and M. Irulappan, "Insertion force analysis of compliantly supported peg-in-hole assembly," *Assembly Automation*, vol. 37, no. 3, pp. 285–295, 2017-08-07Z.
- [10] X. Zhou, G. Zhao, Y. Xing, J. Wu, and Z. Xiong, "Robotic Stacking of Irregular Objects with Load Position Identification and Compensation," in *2023 IEEE 19th International Conference on Automation Science and Engineering (CASE)*. Auckland, New Zealand: IEEE, Aug. 2023, pp. 1–7.
- [11] A. Papavasileiou, G. Michalos, and S. Makris, "Quality control in manufacturing – review and challenges on robotic applications," *International Journal of Computer Integrated Manufacturing*, vol. 38, no. 1, pp. 79–115, Jan. 2025.
- [12] L. Bertscheid, T. Ruhr, and T. Kroger, "Improving Data Efficiency of Self-supervised Learning for Robotic Grasping," in *2019 International Conference on Robotics and Automation (ICRA)*. Montreal, QC, Canada: IEEE, May 2019, pp. 2125–2131.
- [13] A. Robertsson, T. Olsson, R. Johansson, A. Blomdell, K. Nilsson, M. Haage, B. Lauwers, H. Baerdemaeker, T. Brogardh, and H. Brantmark, "Implementation of Industrial Robot Force Control Case Study: High Power Stub Grinding and Deburring," in *2006 IEEE/RSJ International Conference on Intelligent Robots and Systems*. Beijing, China: IEEE, Oct. 2006, pp. 2743–2748.
- [14] I.-C. Hsueh, Y.-H. Lan, D.-H. Lin, C.-H. Huang, and C.-C. Lan, "A compact compliant robot for the grinding of spherical workpieces with high force control accuracy," *Robotics and Computer-Integrated Manufacturing*, vol. 91, p. 102856, Feb. 2025.
- [15] F. Hagelskjær, D. Kraft *et al.*, "Off-the-shelf bin picking workcell with visual pose estimation: A case study on the world robot summit 2018 kitting task," in *2024 21st International Conference on Ubiquitous Robots (UR)*. IEEE, 2024, pp. 145–152.
- [16] F. Hagelskjær, "Good Grasps Only: A data engine for self-supervised fine-tuning of pose estimation using grasp poses for verification," in *2025 IEEE/SICE International Symposium on System Integration (SII)*. Munich, Germany: IEEE, Jan. 2025, pp. 957–964.
- [17] F. Hagelskjær and D. Kraft, "In-hand pose estimation and pin inspection for insertion of through-hole components," in *2022 IEEE 18th International Conference on Automation Science and Engineering (CASE)*. IEEE, 2022, pp. 382–389.
- [18] R. W. Schafer, "What is a savitzky-golay filter? [lecture notes]," *IEEE Signal Processing Magazine*, vol. 28, no. 4, pp. 111–117, 2011.
- [19] F. Pedregosa, G. Varoquaux, A. Gramfort, V. Michel, B. Thirion, O. Grisel, M. Blondel, P. Prettenhofer, R. Weiss, V. Dubourg, J. Vanderplas, A. Passos, D. Cournapeau, M. Brucher, M. Perrot, and E. Duchesnay, "Scikit-learn: Machine learning in Python," *Journal of Machine Learning Research*, vol. 12, pp. 2825–2830, 2011.